Equilibrium sizes and formation energies of small and large Lennard-Jones clusters from molecular dynamics: A consistent comparison to Monte Carlo simulations and density functional theories

Jan Julin,[1,a)] Ismo Napari,[1] Joonas Merikanto,[2] and Hanna Vehkamäki[1]
[1]*Department of Physics, University of Helsinki, P.O. Box 64, FI-00014 Helsinki, Finland*
[2]*School of Earth and Environment, University of Leeds, Leeds LS2 9JT, United Kingdom*

(Received 8 September 2008; accepted 12 November 2008; published online 16 December 2008)

We have performed molecular dynamics simulations of Lennard-Jones argon clusters in equilibrium with a surrounding vapor and combined them with simulations of nucleation events in supersaturated vapor to investigate the dependence of critical cluster size on the vapor density in the cluster size range of 20–300 atoms. The simulations are performed at reduced temperature $T'=0.662$, which with the parameter values of Lennard-Jones argon corresponds to 80 K. We obtain bulk equilibrium values by simulating a planar liquid-vapor interface. In the studied cluster size range, we find a linear relation between critical size ΔN^* and $\Delta\mu^{-3}$, where $\Delta\mu$ is the chemical potential difference between supersaturated vapor and saturated vapor, but the slope of the line is not given by the Kelvin relation of classical nucleation theory. With this relation, along with the known formation energy of the small critical cluster of the nucleation simulations, we proceed to calculate the formation energies for larger critical sizes by integrating the nucleation theorem. We compare the molecular dynamics results to results from Monte Carlo simulations and both perturbative density functional theory and square gradient theory calculations. We find that the molecular dynamics results are in excellent agreement with the density functional and square gradient values. However, the Monte Carlo critical sizes and formation energies are somewhat lower than the molecular dynamics ones. © *2008 American Institute of Physics*. [DOI: 10.1063/1.3040245]

I. INTRODUCTION

One important example of nucleation phenomenon, among other things due to its central role in atmospheric particle formation,[1] is homogeneous nucleation in gas phase, where small liquidlike clusters of molecules appear spontaneously in a metastable vapor. The formation of such clusters is a kinetic process on molecular scale but it can be approached through thermodynamics. Thermodynamic description of gas-liquid nucleation[2,3] amounts to writing the formation free energy of the cluster as a sum of two competing contributions: a negative volume energy representing the energy gained from transfer from a state of higher energy (supersaturated vapor) to a state of lower energy (liquid) and a positive surface energy describing the energy needed to form an interface between the liquid and vapor phases. The cluster has equal probability of growing and shrinking where the competing energy contributions balance. Finding the size and the formation energy of this so-called critical cluster is the main objective of theoretical nucleation research.

To bring the nonextensive part of the system (cluster) within the realm of bulk thermodynamics, one replaces the real cluster with a hypothetical droplet having the properties of bulk liquid in chemical equilibrium with the surrounding vapor. In classical nucleation theory (CNT) it is further assumed that the droplet phase is incompressible with the density of equilibrium bulk liquid ρ_l and the surface tension equals the surface tension of planar interface γ_∞ (capillary approximation). The excess number of particles in the critical nucleus is then given by the Kelvin relation

$$\Delta N^*_{\mathrm{CNT}} = \frac{32\pi\gamma_\infty^3}{3\rho_l^2(\Delta\mu)^3}, \tag{1}$$

where $\Delta\mu=\mu_v-\mu_{v,e}$ is the chemical potential difference between the metastable supersaturated vapor and saturated vapor, and the free energy of formation is

$$W^*_{\mathrm{CNT}} = \tfrac{1}{2}\Delta N^*_{\mathrm{CNT}}\Delta\mu. \tag{2}$$

Formulas (1) and (2) are the working equations in the classical theory of one-component nucleation.

The success of CNT has been somewhat mixed. While CNT gives the correct qualitative picture of nucleation, the quantitative predictions do not compare well with the measurements.[4,5] The nucleation rate (the number of critical clusters appearing in a unit volume and time) calculated using W^*_{CNT} often disagrees with the experimental values by several orders of magnitude. The failure of CNT in this respect has spurred a vast amount of research to find an alternative approach to nucleation. On the other hand, the size of the critical droplet seems to be quite reliably given by $\Delta N^*_{\mathrm{CNT}}$ even for very small clusters. This rather surprising fact has been deduced from experiments,[6] where the size of critical cluster can be obtained by nucleation theorem,[2,3]

[a)]Electronic mail: jan.julin@helsinki.fi.

$$\frac{\partial W^*}{\partial \Delta\mu} = -\Delta N^* \tag{3}$$

or

$$\frac{\partial \ln J}{\partial(\Delta\mu/k_BT)} \approx \Delta N^* + 1, \tag{4}$$

where J is nucleation rate. The right hand side of Eq. (4) is obtained using the CNT expression for the kinetic prefactor in the nucleation rate, but even without assuming any macroscopic bulk properties for the critical cluster, the right hand side of Eq. (4) is approximately ΔN^* with an accuracy of one or two atoms.[6–8] Thus using Eq. (4) to obtain critical sizes from experiments or simulations results in values that are independent of theoretical models and cluster definitions.

Generally, correct critical sizes result in correct supersaturation dependence for the nucleation rate and vice versa, whereas correct critical formation energies result in a correct temperature dependence for the nucleation rate. As CNT manages to predict supersaturation dependence considerably better than temperature dependence, the mixed success of CNT mentioned above is understandable.

Besides the experimental evidence, the correctness of the classical result of Eq. (1) is supported to some extent by theoretical considerations and simulations. McGraw and Laaksonen presented scaling relations for the critical nucleus,[9] basing their derivation on the nucleation theorem (3). With a simplifying assumption (see Ref. 9 for details) they proposed that

$$\Delta N^* = C(T)(\Delta\mu)^{-3} \tag{5}$$

and, by the fact that CNT must be correct at the limit of droplet of infinite radius, the function $C(T)$ should be given by Eq. (1). However, as Koga and Zeng showed,[10] Eq. (5) only represents one term (although the most important one) in a series of powers of $\Delta\mu$. Therefore, there is no *a priori* reason for Eq. (5) to be universally valid. Nevertheless, both density functional theory (DFT) calculations[9,11] and Monte Carlo (MC) simulations[12–14] indicate that the scaling of Eq. (5) is satisfied at least for simple fluids and even the prefactor $C(T)$ is correctly given by the CNT expression (1). A similar conclusion has been made for very small clusters in recent molecular dynamics (MD) simulations.[15] Fluids consisting of long-chained molecules may show some deviation from this rule.[11,16]

With the nucleation theorem (3), the scaling theory of McGraw and Laaksonen leads to another important result,[9] namely, that the formation energy W^* and the corresponding CNT value are related by

$$W^* - W^*_{\mathrm{CNT}} = -D(T). \tag{6}$$

MC simulations lend support to this result.[12–14]

Both DFT and MC methods are subject to some simplifications. DFT is usually applied at the mean-field level which, for example, affects the temperature dependence of surface tension;[17] possible mean-field effects to the scaling of cluster properties are unknown. MC method is a fully molecular-level approach with a proper treatment of interparticle correlations, but it lacks dynamics. Furthermore, here we use a MC method that disregards the interactions between the vapor and the cluster. Differences in MC methodology may also have an effect.[18] MD is in this sense superior to DFT and MC, and it can thus be used to validate the DFT and MC results.

So far, MD has not been used to investigate the scaling relations with the cluster size ranging from tens of particles to hundreds of particles. There are two main reasons for this: first of all, to study the formation of critical clusters out of the vapor phase, time-consuming simulations are needed and even then the size of the critical cluster is less than about 30 molecules.[15,19,20] Stable equilibrium of vapor and cluster can be studied more easily,[21,22] and the equilibrium properties thus achieved (vapor density and cluster density distribution) are equal to those in unstable equilibrium, if the volume of the vapor phase surrounding the cluster is large enough[23] and corrections pertaining cluster fluctuations and translation are neglected.[24] This method, however, does not give information on formation energy, which leaves the scaling law (6) in doubt. Also, to compare the scaling relations with simulation one must know the values for bulk properties of the fluid, which should be obtained from simulations of a planar liquid-vapor interface using exactly the same interaction potential as in cluster simulations.

The purpose of this paper is to study cluster-vapor equilibrium of a simple Lennard-Jones (LJ) system using MD simulations and to study the possible deviations from these MD properties that the simplifications of MC simulations and DFT calculations might cause. First we find out the relation between the cluster size and the density of the surrounding vapor by MD methods and test the validity of the particle number scaling law (5). With a linear scaling found, we proceed to perform actual MD nucleation simulations to obtain a reference point with a known formation energy and then use the scaling with the nucleation theorem to calculate formation energies of larger clusters. All the while, a consistent comparison with MC simulations and DFT calculations is made.

In Sec. II we describe our simulation methods for clusters, nucleation, and bulk equilibrium, and also outline the density functional method. The results are presented in Sec. III. The possible sources of the differences between the simulation methods are discussed, and conclusions are presented in Sec. IV.

II. SIMULATION AND THEORETICAL METHODS

A. MD simulations of cluster-vapor equilibrium and nucleation

The interaction potential in the simulations was a LJ potential, and the parameter values of argon (σ=3.40 Å and ϵ=0.24 kcal/mol) were used. The potential was cut and shifted at 5σ. All of our simulations were performed in a cubic simulation box with periodic boundary conditions, and the MD simulation time step was 6 fs. In the following, the results are reported in reduced units with $\rho' = \rho\sigma^3$, $P' = P\sigma^3/\epsilon$, $\mu' = \mu/\epsilon$, and $\gamma' = \gamma\sigma^2/\epsilon$.

The starting configuration of the simulations of cluster-vapor equilibrium was a cluster containing all the particles

present in the system. As the simulation proceeded, some of the atoms evaporated from the cluster to form a vapor phase, which eventually was in equilibrium with the liquid cluster, the size of which fluctuated around an equilibrium value. When the system had reached equilibrium, we started to collect data from the simulation. This was done after 0.75 ns (125 000 time steps). Total simulation time for a single run was 4.8 ns.

We performed cluster simulations for ten different system sizes, ranging from 65 to 310 particles. Going for even smaller system sizes becomes increasingly difficult, as having a too large simulation box will result in the cluster evaporating completely, yet a too small box would cause the periodic images of the cluster to interfere with each other, and the averaged density would not attain a constant value close to the box boundary. For the sizes available, the starting configuration was taken from the Cambridge cluster database[25] (that is, for 310 particles and sizes smaller than 150 particles), and for the rest we created the starting cluster ourselves. The number of atoms that make up the vapor phase around the cluster is small, so some slight variation in the value of the vapor density from different simulation runs is inevitable. For this reason, 20 runs were performed for each system size in order to obtain an average density profile. The density profile was calculated by dividing the system to spherical layers 0.1σ thick. The equilibrium size was obtained from the density profile by integration,

$$\Delta N^* = 4\pi \int_0^\infty dr r^2 (\rho(r) - \rho_v), \tag{7}$$

where ρ_v is the density of the homogeneous vapor. We also calculated the cluster size according to the simple Stillinger definition.[26] The effect of cluster definition is discussed in Sec. IV.

Every time step, the center of mass of the system was moved to the center of the simulation box. As most of the atoms in the system belong to the cluster, the center of mass of the system is quite accurately also the center of mass of the cluster. Therefore the kinetic energy due to the translation of the cluster as a whole was nearly nonexistent. We took no steps to prevent the cluster from rotating, but kept track of the rotational energy of the cluster. The rotational energy was fairly insignificant compared to the total kinetic energy of the cluster, being less than 2% for even the smallest system and even less than 0.5% for the largest.

We also performed gas-phase simulations of the supersaturated vapor and the subsequent nucleation event (called hereafter "direct nucleation simulations"). In these simulations we ran the simulations first at a higher temperature to achieve a random starting configuration, then quenched the system to the supersaturated state. The simulation then continued until nucleation was observed and the cluster had grown to a size of 200 particles, or if no nucleation has occurred within 100 ns of simulation time, the simulation was terminated.

Nucleation rate was determined from the direct nucleation simulations by the mean first passage time (MFPT) method introduced by Wedekind *et al.*[19] The obtained nucleation rates along with other data related to the direct nucleation simulations are collected in Table I. Using a different method to obtain the nucleation rate, for example, the threshold method of Yasuoka and Matsumoto,[27] may result in somewhat lower nucleation rates.[28] The MFPT method requires sufficient statistics, so we performed 50 runs for each of the four different systems of our direct nucleation simulations (see Table I). The number of atoms in the system was chosen so that the deviation in nucleation rate caused by finite-size effects would be no more than 10%.[29]

TABLE I. Vapor densities (ρ_v') and number of atoms (N_{total}) of the systems used in the direct nucleation simulations and the nucleation rates and the Stillinger critical sizes obtained by the MFPT method.

ρ_v'	N_{total}	J'	ΔN^*
0.0220	500	6.3×10^{-8}	32.2
0.0197	640	2.1×10^{-8}	33.7
0.0174	870	3.3×10^{-9}	36.6
0.0151	1300	5.4×10^{-10}	33.7

The critical cluster size is obtained from the direct nucleation simulations by using the nucleation theorem in the form of Eq. (4). Plotting a nucleation rate isotherm, with the nucleation rates and chemical potentials calculated for the four different direct simulation systems, the critical size is found from the slope of the $\ln J(\Delta\mu)$ line. The resulting critical size is practically independent of the chosen cluster definition, as the nucleation rate obtained with the MFPT method is quite insensitive to the cluster definition.[30] A value for the critical size can also be extracted directly from the MFPT fit (see Table I),[19] but this naturally depends on the choice of the cluster definition (here the Stillinger definition). It has been previously shown that, compared to the critical size obtained from the nucleation theorem, the Stillinger definition overestimates the size of the critical cluster.[15,30] This is also seen in the present work and discussed in Sec. IV.

The temperature of the simulated systems was kept constant by coupling the systems to a Berendsen thermostat,[31] in which the velocity of each particle is scaled by a factor that depends on the current kinetic temperature. For direct nucleation simulations it has been shown that the choice of the thermostatting method is not a critical issue in obtaining the nucleation rate.[20,32] For the cluster simulations the Berendsen thermostat managed to keep the cluster well at the desired temperature, but the vapor temperature could change from one run to another and be below, above, or sometimes even at the target temperature. However, we found no clear correlation with the vapor temperature and density, so even though after the 20 runs for each system size the vapor temperature was on average slightly above the desired temperature, it is most likely not a significant error source.

All simulations were performed at temperature $T' = k_B T/\epsilon = 0.662$ which corresponds to 80 K when the LJ parameters of argon are used. This is approximately at the triple point of the system, considering that the triple point of LJ fluid with full potential is $T' = 0.694$.[33]

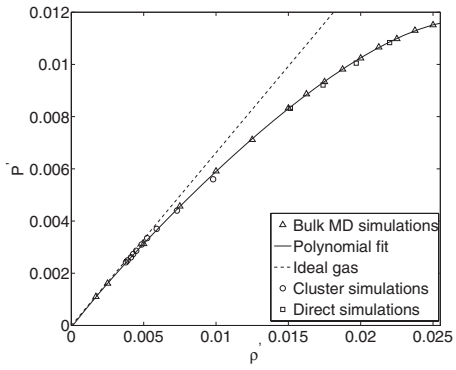

FIG. 1. The simulated pressure-density correlation. The triangles denote the points to which the sixth order polynomial (solid line) is fitted. The circles denote the cluster simulations and the squares the direct nucleation simulations. The dashed line is the ideal gas equation of state.

B. MD simulations of bulk equilibrium

A meaningful comparison of cluster simulations with CNT requires a consistent set of bulk equilibrium values, namely, chemical potential, liquid density, and surface tension. In view of the recent progress and findings concerning simulations of surface tension and metastable vapor,[34,35] together with the fact that the bulk values depend much on the potential cutoff,[36] we decided to simulate the bulk values for the particular system under study instead of approximating them from literature data.

The vapor in many of our cluster simulations is in a highly supersaturated state. Large errors are then expected if vapor pressure is calculated from ideal gas law. We therefore simulated metastable vapor along the isotherm at $T'=0.662$ at several densities up to $\rho_v'=0.025$ and measured the vapor pressure from the pressure virial to build up a pressure-density correlation. The method is akin to that by Linhart *et al.*:[34] starting from a configuration with the atoms located at evenly spaced grid points in a periodic box, 1000 atoms at vapor density were simulated for a fixed period of time or until nucleation onset. The vapor was first allowed to equilibrate for 100 ps and data were then collected up to 1 ns. At high supersaturations the data collecting period was shorter and several simulation runs were needed to find a case where the nucleation did not start too soon. This simulation method allows for a natural clusterization in the vapor and yields more realistic pressure at high density region compared to many published equations of state;[34] however, we did not extend our simulations to densities very close to spinodal conditions because they were not needed in the present work. The resulting pressure-density correlation was fitted to a sixth order polynomial and chemical potential was obtained by integration from Gibbs–Duhem equation.

Figure 1 shows the polynomial fit along with the simulated points that it was fitted to. Also shown are the points acquired from the cluster simulations, the vapor pressure being calculated using the Irving–Kirkwood definition of the pressure tensor. We note that although there is no unique way to calculate the pressure tensor for droplets,[37] the different definitions give consistent results for homogeneous bulk (in this case the vapor surrounding the cluster). The four points corresponding to the four direct nucleation simulation system sizes also appear in the figure, the pressure here obtained from the period before the nucleation onset by calculating the pressure virial. As can be seen, the vapor in both cluster simulations and direct nucleation simulations obeys the same pressure-density correlation well.

TABLE II. Values for equilibrium vapor density, surface tension, and liquid density from different simulation methods. The error given in the brackets for the MD values is the standard deviation in units of the last digits.

	$\rho_{v,e}'$	γ_∞'	ρ_l'
MD	0.001 43(9)	1.107(8)	0.8524(1)
MC	0.001 43	1.115	···

The equilibrium vapor density, liquid density, and surface tension were obtained from simulations of planar liquid-vapor interface. First, a liquid slab containing 3332 atoms was placed at the center of a simulation box with dimensions of $49\times49\times186.15$ Å^3, the interface being perpendicular to the z direction. The vapor phase was then allowed to form and the system to equilibrate for 1 ns and after that data were collected for 5 ns. Dividing the simulation box into 0.1σ thick slabs parallel to the interface we collected density and pressure profiles. The surface tension is then

$$\gamma_\infty = \frac{1}{2}\int_{-\infty}^{\infty}(p_N - p_T)dz, \tag{8}$$

where p_N and p_T are the normal and transverse components of the pressure tensor, respectively (with Kirkwood–Buff definition of the pressure tensor). The results used here are averages of ten simulation runs. The values are shown in Table II along with corresponding values from MC simulations. The agreement of these values is discussed in Sec. III.

C. MC simulations

We used single cluster MC simulations to calculate the cluster free-energy characteristics, the equilibrium vapor pressure, and bulk liquid surface tension for the same LJ interaction potential that was used in the MD simulations. Previously, similar MC simulations have been used to study nucleation in argon and water systems, and full simulation details are presented elsewhere.[18,38] We defined the clusters according to the Stillinger cluster definition, where we selected the characteristic Stillinger radius to be $r_s=1.39\sigma$; our previous studies with the full LJ potential have shown that for the selected value of r_s, the free energy of the smallest cluster is consistent with the known virial coefficients.[39] We studied one cluster at a time with a fixed number of particles in a canonical Metropolis simulation, and for each cluster size the average grand canonical growth and decay rates, $\overline{G_N}$ and $\overline{D_N}$, respectively, were calculated. The interactions between the simulated cluster and the clusters in the surrounding vapor were omitted. It can be shown from statistical mechanics of noninteracting clusters that the cluster work of formation with respect to bulk liquid with a chemical potential μ_l can be obtained from

$$W_{N,\mathrm{MC}} = -k_B T \sum_{N'=2}^{N} \ln\left(\frac{\bar{G}_{N'-1}(\mu_l)}{\bar{D}_{N'}(\mu_l)}\right) - N\Delta\mu_1, \tag{9}$$

where the subscript 1 describes the monomers, $\Delta\mu_1 = \mu_1 - \mu_1^e \simeq \Delta\mu$, and the work of cluster formation W_N corresponds to a cluster distribution of the form

$$C_N = C_1^e \exp(-W_N/k_B T), \tag{10}$$

where C_1^e is the monomer number density in saturated vapor. In CNT the corresponding expression for the cluster work of formation is given by

$$W_{N,\mathrm{CNT}} = A_1 N^{2/3}\gamma_\infty - N\Delta\mu, \tag{11}$$

where A_1 is the spherical monomer surface area. The value for A_1 was obtained from the bulk liquid density calculated with MD simulation. In line with our previous studies,[14,39] we found that for clusters larger than a threshold size $N^{\mathrm{thr}}=30$ the difference $\delta W_{N,\mathrm{MC}} = W_{N,\mathrm{MC}} - W_{N-1,\mathrm{MC}}$ becomes linear with respect to the change in cluster spherical surface area, as expected from the CNT. We calculated the bulk liquid surface tension γ_∞ from the slope of the $\delta W_{N,\mathrm{MC}}$ line. The saturated vapor density $\rho_v^e = \rho_1^e + \rho_2^e + \cdots$ was obtained by locating the chemical potential for which $\delta W_{N,\mathrm{MC}}$ approached zero as $N \to \infty$. The obtained values for γ_∞ and ρ_v^e both from MC and MD simulations are in a very good agreement as shown in Table II. Therefore, our MC simulations support the McGraw–Laaksonen scaling laws for clusters larger than N^{thr}. The scaling constant $D(T)$ was obtained from

$$D(T) = A_1\gamma_\infty - \sum_{N=2}^{N^{\mathrm{thr}}} [\delta W_{N,\mathrm{CNT}} - \delta W_{N,\mathrm{MC}}]. \tag{12}$$

In this study, we found $D(T) = 16.8 k_B T$. This value is close to values found in previous MC studies with a full LJ interaction potential.[14,40]

D. Density functional methods

In DFT the grand potential of the system $\Omega[\rho(\mathbf{r})]$ is expressed as a functional of the particle number density distribution $\rho(\mathbf{r})$. Here we consider two popular mean-field forms of $\Omega[\rho(\mathbf{r})]$. In a perturbative approach to DFT (PDFT) the grand-potential functional can be written as[41]

$$\Omega[\rho(\mathbf{r})] = \int d\mathbf{r} f_h(\rho(\mathbf{r})) + \frac{1}{2}\int\int d\mathbf{r} d\mathbf{r}' \phi^{\mathrm{LJ}}(|\mathbf{r}-\mathbf{r}'|) \times \rho(\mathbf{r})\rho(\mathbf{r}') - \mu\int d\mathbf{r}\rho(\mathbf{r}). \tag{13}$$

Here the repulsive part of the LJ potential $\phi^{\mathrm{LJ}}(|\mathbf{r}-\mathbf{r}'|)$ is replaced with a hard-sphere potential and $f_h(\rho)$ is the known Helmholtz free-energy density of the uniform hard-sphere system with density ρ. An even simpler form of grand-potential functional is obtained in the so-called square gradient theory (SGT),[42,43]

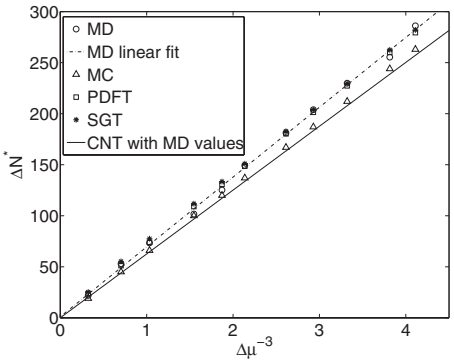

FIG. 2. The MD, MC, PDFT, and SGT critical sizes as a function of $(\Delta\mu)^{-3}$. The circles represent the MD simulations with the smallest critical size corresponding to the direct nucleation simulations. The triangles denote the MC, squares the PDFT, and stars the SGT critical sizes in corresponding vapors. The solid line is the CNT line with the surface tension from the MD planar interface simulations.

$$\Omega[\rho(\mathbf{r})] = \int \left\{ f_0(\rho(\mathbf{r})) + \frac{c}{2}[\nabla\rho(\mathbf{r})]^2 - \mu\rho(\mathbf{r}) \right\} d\mathbf{r}, \tag{14}$$

where $f_0(\rho)$ is the free-energy density of the uniform fluid. In this work we assume $f_0(\rho)$ given by the Peng–Robinson equation of state.[44] The influence parameter c is related to the direct correlation function[45] but treated here as a constant.

Minimization of the grand potential $\delta\Omega[\rho(\mathbf{r})]/\delta\rho(\mathbf{r}) = 0$ yields an Euler–Lagrange equation from which the equilibrium density distribution can be solved by numerical means. By writing the equation in planar geometry a liquid-vapor interface can be studied, whereas spherical geometry is suitable for droplets surrounded by a vapor phase. In PDFT the free-energy functional for uniform fluid gives the equation of state. All the properties needed in this work, for example, vapor pressure, surface tension, and critical cluster size, are obtained from DFT in a consistent manner.

Since the density functional methods described above represent rather low-level approach to fluids compared to MC and MD simulations where the interparticle correlations are properly taken into account, a meaningful comparison to simulation entails some adjustment of the parameters in DFT. Applying the ideas of Ref. 46 in PDFT we fit the LJ parameters (ϵ and σ) and the hard-sphere diameter to obtain the same equilibrium vapor pressure, bulk liquid density, and surface tension as in planar MD simulations. In SGT the MD equilibrium vapor pressure and liquid density are used to obtain the two parameters of the Peng–Robinson equation of state, and the influence parameter c is adjusted so that the MD value of surface tension is obtained.

III. RESULTS

A. Cluster sizes

We now proceed to plot our resulting cluster sizes as a function of $\Delta\mu^{-3}$. These plots are shown in Fig. 2, and we do indeed get a linear relation also for the MD results as the scaling relation (5) suggests. The ten largest MD points correspond to the cluster simulations where the cluster size is obtained from the density profile. The MD point in Fig. 2

corresponding to the smallest cluster size ($\Delta N^*=22$) is obtained from the direct nucleation simulations by using the nucleation theorem. This turns out to be considerably smaller than what one would get directly from the MFPT fit using the Stillinger cluster definition, which indicates that $\Delta N^*=34$.

Even though the MD results follow a linear scaling, the slope of the line is not given by the Kelvin relation, Eq. (1). This is clearly seen in Fig. 2 where the CNT line is plotted with the values for surface tension and liquid density from the planar interface simulations. Also, the linear fit to the MD results does not pass exactly through the origin; however, a slight change in the equilibrium vapor density (one comfortably within the uncertainty reported in Table II) would be enough to make the line pass through the origin.

The critical sizes from the PDFT calculations agree remarkably well with the MD results, as do the SGT values. The MC critical sizes are of similar magnitude, but somewhat smaller than the MD ones for any given vapor. As the vapor pressure (or density) is an external parameter in MC simulations, we have used the same $\mu(\rho)$ correlation for consistent comparison of MD and MC simulations.

The MC simulations yield a value for equilibrium vapor pressure that is in excellent agreement with the average value from the MD simulations (see Table II). The values for the surface tension do not agree quite as well, but the MC value is still within the uncertainty limits of the MD value. As the MC surface tension is determined with the aid of CNT,[14,39] a CNT line with the MC value for surface tension follows the MC points of Fig. 2 and is thus omitted from the figure.

B. Formation energies

As we now have the critical cluster size as a function of chemical potential from MD, we are able to calculate the formation free energies W^* by integrating the nucleation theorem, Eq. (3). Instead of using the actual simulated $(\Delta\mu, \Delta N^*)$ points, which necessarily include some statistical uncertainty, we use the linear fit shown in Fig. 2. The method based on the nucleation theorem requires some reference point with a known formation energy to obtain an absolute value of W^*. The obvious choice is then the point obtained from the direct nucleation simulations, as unlike the cluster-vapor simulations, the direct nucleation simulations provide us the nucleation rate

$$J = K \exp(-W^*/k_BT), \tag{15}$$

from where W^* can be readily solved. The prefactor K is written in CNT as[3,47–49]

$$K = \beta C_1^e Z, \tag{16}$$

where Z is the Zeldovich nonequilibrium factor

$$Z = \sqrt{\frac{\gamma_\infty}{k_BT}} \frac{v_l}{2\pi r^{*2}}, \tag{17}$$

where v_l is the equilibrium molecular volume of bulk liquid and r^* is the radius of the critical cluster and β is the condensation coefficient given by

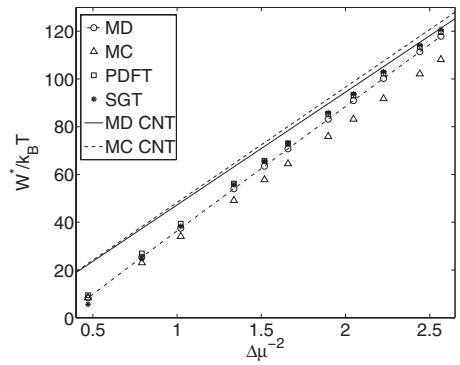

FIG. 3. The formation energies as a function of $(\Delta\mu)^{-2}$. The lowest MD formation energy is the reference value obtained from nucleation simulations, with the rest of the circles corresponding to the vapors surrounding the simulated clusters. The triangles denote the MC, squares the PDFT, and stars the SGT critical sizes in corresponding vapors. Also plotted are the CNT predictions with surface tensions from MD cluster simulations (solid line) and MC simulations (dashed line).

$$\beta = SP_{v,e}\sqrt{\frac{6}{k_BT}}\left(\frac{3}{4\pi}\right)^{1/6}\left(\frac{1}{\Delta N^* m}+\frac{1}{m}\right)^{1/2} \times((\Delta N^* v_l)^{1/3}+v_l^{1/3})^2, \tag{18}$$

where S is the saturation ratio, $P_{v,e}$ is equilibrium vapor pressure, and m is the mass of the atom.

In Fig. 3 we have plotted the formation energies that correspond to the vapors of Fig. 2. The agreement between MD results and PDFT (as well as SGT) calculations, while still quite good, is not as good as it is for the critical sizes. However, this is not an indication that the PDFT and SGT results would be incompatible with the nucleation theorem. While the difference between the MD and DFT critical sizes is small, the DFT clusters do not follow exactly the same linear relation as the MD ones, a difference that is somewhat magnified when calculating the formation energies. Even the reference MD formation energy differs slightly from the PDFT and SGT energies calculated at the same vapor. Furthermore, the MD formation energies are affected by an uncertainty in the reference value. This arises mainly from the simulated nucleation rates and for a smaller part from the kinetic prefactor in the expression of the nucleation rate. However, this should at most account for a change of $1.5k_BT$ in the formation energy.

MC simulations yield the formation energies directly as a simulation result. The MC values are also plotted in Fig. 3. The MD values are somewhat higher than the corresponding MC values for the vapors considered here, although at the vapor corresponding to the reference MD value, the MC and MD energies are practically the same. In agreement with the McGraw–Laaksonen scaling of Eq. (6), Fig. 3 shows that there is a constant difference between the simulated MC formation energies and the CNT prediction, as has been previously shown.[14] For MD the difference is not constant, but this is expected since for Eq. (6) to be valid would require the MD critical size to be equal to the CNT one, which is not the case.

IV. DISCUSSION AND CONCLUSIONS

Despite the good agreement that we have between MD and MC values for bulk equilibrium vapor density and surface tension, there is a noticeable difference in the critical cluster size and formation energy obtained from MD and MC with the MC values being lower than the MD values for both properties. Excluding the region of relatively dense vapors of the direct nucleation simulations and the smaller systems of the cluster simulations, at lower supersaturations the MC critical sizes tend to be about 7% smaller (when comparing to the linear fit of Fig. 2) and formation energies 8%–9% smaller than the MD values. There are at least three conceivable causes for the differences. First, the MC simulations lack a vapor phase, and as such lack cluster-vapor interactions, which is bound to cause some difference compared to MD simulations. However, in LJ vapor-liquid nucleation both McGraw–Laaksonen scaling laws have also found support from grand canonical MC simulations that include the cluster-vapor interactions.[12,13,40] It is interesting to note that simple arguments indicate a decrease in cluster size and formation energy when cluster-vapor interactions are accounted for,[50,51] which in our case increases the discrepancy between MD and MC. Second, there are known differences in regard to critical cluster size and formation energy between different MC simulation methods. Instead of using growth/decay method, discrete summation method would have resulted in a somewhat larger critical cluster with higher formation energy in a given vapor[18] and thus increased the slope of the MC line in Figs. 2 and 3. However, this does not prove that the values from the discrete summation method would be in agreement with the MD values. Finally, some differences might be caused by the fact that cluster translation is prevented in the cluster-vapor simulations while in MC one integrates also over the momentum coordinates. However, the movement of the cluster in direct nucleation simulations is unrestricted, and the point obtained from these simulations still follows the same linear relation as the points from cluster-vapor simulations in Fig. 2, which would imply that the translational restriction for the cluster does not result in a very noticeable effect. Considering these facts, the discrepancies between MD and MC are still an open question.

Independent of simulation method, one important factor affecting the cluster size is the cluster definition. If the vapor phase around the cluster is present, as in MD simulations, integration of the density profile [Eq. (7)] should constitute a physically sound and thermodynamically consistent method to determine the size of the cluster. Density profile unambiguously distinguishes the two equilibrium states needed for thermodynamically meaningful use of nucleation theorem: the homogeneous supersaturated vapor and the density fluctuation above the vapor (cluster). An alternative method to determine the cluster size is by the Stillinger definition: a particle belongs to a cluster if it has at least one neighbor within a preset distance. We used $r_s=1.5\sigma$ for the Stillinger radius in the MD simulations. Simply keeping track of the Stillinger defined size of the largest cluster in the simulation box throughout the simulation yields a value for the cluster size. The Stillinger cluster sizes in cluster-vapor simulations were only one to two atoms bigger than cluster sizes obtained from the density profile. We performed some MD runs with different values for the Stillinger radius, but, for example, the effect a 0.1σ change of r_s had on the cluster size was negligible.

In MC simulations the Stillinger radius was $r_s=1.39\sigma$ (see Sec. II C). We carried out additional simulations to study the sensitivity of the results to changes in the applied Stillinger radius. Compared to simulations with $r_s=1.39\sigma$ the critical cluster size increased only by approximately 1% with $r_s=1.5\sigma$, while the critical formation work was practically unchanged. With $r_s=1.5\sigma$ we obtained $D(T)=17.6k_BT$ and $\gamma'_\infty=1.119$. Altogether, the differences in the cluster definition are not able to explain the dissimilar critical cluster sizes from MD and MC cluster simulations.

In contrast to the MD cluster-vapor simulations, in the direct nucleation simulations the Stillinger cluster (that is, the cluster with the size obtained directly with the MFPT method) was considerably bigger (34 atoms) than the one obtained with the nucleation theorem (22 atoms). This is not necessarily an inconsistent result with the cluster-vapor simulations because in our direct nucleation simulations the critical cluster size is so small that it likely has a more diffuse and fragmented structure than the approximately spherical and well-defined larger clusters. The outlying atoms in the small cluster are easily included in the cluster by the Stillinger criterion but contribute little to the density profile. It is probable that this difference becomes more pronounced as the cluster size decreases. In their recent MD simulations, Wedekind *et al.*[15] found that compared to the nucleation theorem result, the Stillinger size was larger by a factor of approximately 2 for clusters of 5–13 atoms, as determined from the nucleation theorem. Further confidence in the compatibility of cluster sizes from nucleation theorem and from the density profile is given by the fact that the point from direct nucleation simulations lies on the same line as the points from cluster-vapor simulations in Fig. 2, whereas the Stillinger cluster would be high above the line. The divergence of critical cluster size on approach to spinodal is expected in the mean-field DFT (Ref. 52) (although only occurring when $W^*<k_BT$) but there is no evidence of such behavior in MD simulations as $W^*\rightarrow 0$. Also, as the cluster size in direct MD simulation conforms to the same linear scaling as the clusters in the equilibrium cluster-vapor simulations, it is apparent that the size and energetics of the clusters in these two approaches are not fundamentally different.

Both the PDFT and square gradient theory agree remarkably well with the MD simulations. Our DFT calculations rely on a fitting procedure by which the bulk values of the fluid are the same in DFT and MD. This approach seems highly successful because the cluster sizes are practically identical in DFT and MD, and the formation energies only differ about $2k_BT$ with PDFT being somewhat closer to MD values than SGT. In nucleation rate this means a difference of just under one order of magnitude. The close agreement of nucleation properties between MD and DFT is not at all obvious because while the surface tensions in MD and DFT are identical, the planar density profiles are not. Also the planar density profile significantly differs from the droplet density

profile especially near the cluster edge,[53] but, apparently, these differences are correctly accounted for in the mean-field level. When the fitting scheme is used, the PDFT is not sensitive to the choice of interaction potential, and instead of LJ potential Yukawa potential might be used.[46] It should also be noted that in SGT the interaction potential is not explicitly defined. It is probable that the density functional methods would not work so well for fluids consisting of, for example, polar molecules.[46]

Although a linear scaling is found for cluster sizes in the size range considered in this study, this does not mean that the same scaling would apply for clusters of all sizes, and the Kelvin equation would thus not be valid even when $\Delta N^* \to \infty$. In fact, we only see a small part of the $\Delta N^*(\Delta\mu^{-3})$ curve which appears locally linear. When the cluster is very large (of the order of 10^6 atoms) the Kelvin limit is correctly approached, as verified by DFT calculations.[10]

In conclusion, the MD simulations suggest a linear scaling of critical sizes as a function of $\Delta\mu^{-3}$ at least for sizes ranging from 20 to 300 atoms. While the values agree well with both DFT and square gradient theory, and reasonably well with MC simulations, the slope of the line is not given by the Kelvin relation. From this it follows that we do not find a constant difference between CNT predictions for the formation energies and MD formation energies calculated with the aid of the nucleation theorem.

It should be noted that the discussion and conclusions above are based on results at just one temperature close to the triple point. At higher temperatures the scaling may have a nonlinear form also in the size range studied here, for example, due to markedly different properties of the supersaturated vapor or non-negligible fluctuations of phase boundaries.

[1] M. Kulmala, H. Vehkamäki, T. Petäjä, M. Dal Maso, A. Lauri, V.-M. Kerminen, W. Birmili, and P. H. McMurry, J. Aerosol Sci. **35**, 143 (2004).
[2] D. Kashchiev, *Nucleation: Basic Theory with Applications* (Butterworth-Heinemann, Oxford, 2000).
[3] H. Vehkamäki, *Classical Nucleation Theory in Multicomponent Systems* (Springer, Berlin, 2006).
[4] V. I. Kalikmanov, J. Wölk, and T. Kraska, J. Chem. Phys. **128**, 124506 (2008).
[5] J. A. Fisk, M. M. Rudek, J. L. Katz, D. Beiersdorf, and H. Uchtmann, Atmos. Res. **46**, 211 (1998).
[6] Y. Viisanen, R. Strey, and H. Reiss, J. Chem. Phys. **99**, 4680 (1993).
[7] D. Kashchiev, J. Chem. Phys. **76**, 5098 (1982).
[8] D. W. Oxtoby and D. Kashchiev, J. Chem. Phys. **100**, 7665 (1994).
[9] R. McGraw and A. Laaksonen, Phys. Rev. Lett. **76**, 2754 (1996).
[10] K. Koga and C. Zeng, J. Chem. Phys. **110**, 3466 (1999).
[11] I. Napari and A. Laaksonen, J. Chem. Phys. **126**, 134503 (2007).
[12] B. Chen, J. I. Siepmann, K. J. Oh, and M. L. Klein, J. Chem. Phys. **115**, 10903 (2001).
[13] P. R. ten Wolde and D. Frenkel, J. Chem. Phys. **109**, 9901 (1998).
[14] J. Merikanto, E. Zapadinsky, A. Lauri, and H. Vehkamäki, Phys. Rev. Lett. **98**, 145702 (2007).
[15] J. Wedekind, J. Wölk, D. Reguera, and R. Strey, J. Chem. Phys. **127**, 154515 (2007).
[16] B. Chen, J. I. Siepmann, K. J. Oh, and M. L. Klein, J. Chem. Phys. **116**, 4317 (2002).
[17] J. Rowlinson and B. Widom, *Molecular Theory of Capillarity* (Clarendon, Oxford, 1989).
[18] A. Lauri, J. Merikanto, E. Zapadinsky, and H. Vehkamäki, Atmos. Res. **82**, 489 (2006).
[19] J. Wedekind, R. Strey, and D. Reguera, J. Chem. Phys. **126**, 134103 (2007).
[20] J. Julin, I. Napari, and H. Vehkamäki, J. Chem. Phys. **126**, 224517 (2007).
[21] S. M. Thompson, K. E. Gubbins, J. P. R. B. Walton, R. A. R. Chantry, and J. S. Rowlinson, J. Chem. Phys. **81**, 530 (1984).
[22] M. Salonen, I. Napari, and H. Vehkamäki, Mol. Simul. **33**, 245 (2007).
[23] V. Talanquer and D. W. Oxtoby, J. Chem. Phys. **100**, 5190 (1994).
[24] D. Reguera and J. M. Ruby, J. Phys. Chem. **115**, 7100 (2001).
[25] D. Wales, J. P. K. Doyle, A. Dullweber, M. P. Hodges, F. Y. Naumkin, F. Calvo, J. Hernández-Rojas, and T. F. Middleton, http://www-wales.ch.cam.ac.uk/CCD.html.
[26] F. H. Stillinger, J. Chem. Phys. **38**, 1486 (1963).
[27] K. Yasuoka and M. Matsumoto, J. Chem. Phys. **109**, 8451 (1998).
[28] F. Römer and T. Kraska, J. Chem. Phys. **127**, 234509 (2007).
[29] J. Wedekind, D. Reguera, and R. Strey, J. Chem. Phys. **125**, 214505 (2006).
[30] J. Wedekind and D. Reguera, J. Chem. Phys. **127**, 154516 (2007).
[31] H. J. C. Berendsen, J. P. M. Postma, W. F. van Gunsteren, A. DiNola, and J. R. Haak, J. Chem. Phys. **81**, 3684 (1984).
[32] J. Wedekind, D. Reguera, and R. Strey, J. Chem. Phys. **127**, 064501 (2007).
[33] E. A. Mastny and J. J. de Pablo, J. Chem. Phys. **127**, 104504 (2007).
[34] A. Linhart, C.-C. Chen, J. Vrabec, and H. Hasse, J. Chem. Phys. **122**, 144506 (2005).
[35] P. Orea, J. López-Lemus, and J. Alejandre, J. Chem. Phys. **123**, 114702 (2005).
[36] A. Trokhymchuk and J. Alejandre, J. Chem. Phys. **111**, 8510 (1999).
[37] P. Schofield and J. R. Henderson, Proc. R. Soc. London, Ser. A **379**, 231 (1982).
[38] J. Merikanto, H. Vehkamäki, and E. Zapadinsky, J. Chem. Phys. **121**, 914 (2004).
[39] J. Merikanto, E. Zapadinsky, A. Lauri, I. Napari, and H. Vehkamäki, J. Chem. Phys. **127**, 104303 (2007).
[40] B. Chen, H. Kim, S. J. Keasler, and R. B. Nellas, J. Phys. Chem. B **112**, 4067 (2008).
[41] X. C. Zeng and D. W. Oxtoby, J. Chem. Phys. **94**, 4472 (1991).
[42] J. W. Cahn and J. E. Hilliard, J. Chem. Phys. **28**, 258 (1958).
[43] J. W. Cahn and J. E. Hilliard, J. Chem. Phys. **31**, 688 (1959).
[44] D.-Y. Peng and D. B. Robinson, Ind. Eng. Chem. Fundam. **15**, 59 (1976).
[45] H. T. Davis, *Statistical Mechanics of Phases, Interfaces, and Thin Films* (VCH, New York, 1996).
[46] R. M. Nyquist, V. Talanquer, and D. W. Oxtoby, J. Chem. Phys. **103**, 1175 (1995).
[47] J. Zeldovich, Zh. Eksp. Teor. Fiz. **12**, 525 (1942).
[48] S. Chapman and T. G. Cowling, *The Mathematical Theory of Non-Uniform Gases* (Cambridge University Press, Cambridge, 1970).
[49] S. K. Friedlander, *Smoke, Dust and Haze* (Wiley, New York, 1977).
[50] K. J. Oh and X. C. Zeng, J. Chem. Phys. **112**, 294 (2000).
[51] B. Senger, P. Schaaf, D. S. Corti, R. Bowles, D. Pointu, J.-C. Voegel, and H. Reiss, J. Chem. Phys. **110**, 6438 (1999).
[52] G. Wilemski and J.-S. Li, J. Chem. Phys. **121**, 7821 (2004).
[53] J. Hrubý, D. G. Labetski, and M. E. H. van Dongen, J. Chem. Phys. **127**, 164720 (2007).